Borophene

International Edition: DOI: 10.1002/anie.201800087
German Edition: DOI: 10.1002/ange.201800087

Universal Scaling of Intrinsic Resistivity in Two-Dimensional Metallic Borophene

*Jin Zhang[+], Jia Zhang[+], Liujiang Zhou, Cai Cheng, Chao Lian, Jian Liu, Sergei Tretiak, Johannes Lischner, Feliciano Giustino, and Sheng Meng**

Abstract: *Two-dimensional boron sheets (borophenes) have been successfully synthesized in experiments and are expected to exhibit intriguing transport properties. A comprehensive first-principles study is reported of the intrinsic electrical resistivity of emerging borophene structures. The resistivity is highly dependent on different polymorphs and electron densities of borophene. Interestingly, a universal behavior of the intrinsic resistivity is well-described using the Bloch–Grüneisen model. In contrast to graphene and conventional metals, the intrinsic resistivity of borophenes can be easily tuned by adjusting carrier densities, while the Bloch–Grüneisen temperature is nearly fixed at 100 K. This work suggests that monolayer boron can serve as intriguing platform for realizing tunable two-dimensional electronic devices.*

The resistivity of metals originating from electron–phonon (e-ph) interactions (that is, their intrinsic resistivity $\rho_{e\text{-}ph}$) is an important fundamental quantity in condensed-matter physics and materials science. At finite temperatures, scattering of electrons by phonons is generally the dominant source of resistivity. In a typical three-dimensional metal with a large Fermi surface, $\rho_{e\text{-}ph}$ is proportional to the temperature T at high T, a consequence of the bosonic nature of the phonons.[1] Below a critical temperature, the resistivity is expected to decrease more rapidly following the relation $\rho_{e\text{-}ph} \sim T^5$. In a two-dimensional (2D) conductor, the low-temperature $\rho_{e\text{-}ph}$ is proportional to T^4 owing to the reduced dimensionality. The transition point between high- and low- temperature regimes is determined by the Debye temperature (Θ_D) at which all phonon modes are excited to scatter carriers. However, in systems with a low electron density or small Fermi surface, the low-temperature behavior of intrinsic resistivity can be well described by the Bloch–Grüneisen model[1] with the characteristic the Bloch–Grüneisen temperature:

$$\Theta_{BG} = 2\hbar v_s k_F / k_B \quad (1)$$

where k_F denotes the Fermi wave vector and vs., $\hbar$, and k_B are the sound velocity, reduced Plank constant, and Boltzmann constant, respectively.[2] Generally, the temperature Θ_{BG} is much smaller than Θ_D in low-density electron gas.

As a semimetal with the largest known electrical conductivity, graphene provides a textbook example for transport properties in 2D systems.[3] The low-temperature $\rho_{e\text{-}ph}$ of graphene is proportional to T^4, while at high temperatures $\rho_{e\text{-}ph}$ varies linearly with T. The transition point is determined by the Θ_{BG} as a consequence of the point-like Fermi surface of graphene.[4] Because of its dependence on k_F, the Θ_{BG} of graphene changes drastically by varying the carrier density or Fermi energy. Previous experiments[3a] by Efetov and Kim have confirmed that Θ_{BG} can change by almost an order of magnitude by applying a gate voltage. Park et al. have demonstrated the relative role of the phonon modes as well as the microscopic nature of e-ph interactions in $\rho_{e\text{-}ph}$.[3b] However, the absolute value of $\rho_{e\text{-}ph}$ in graphene (1.0 μΩ cm at 300 K) is not sensitive to the applied external carrier densities, further limiting potential applications of graphene in highly-tunable nanodevices.

In contrast to graphene, 2D boron sheets, known as borophenes, have a variety of polymorphs.[5] Recently, several borophene phases have been synthesized on Ag surfaces, for example, β_{12}, χ_3, and triangle sheets.[6] All experimentally realized borophenes exhibit intrinsic metallic properties, providing an ideal platform to explore the transport properties of 2D metals, a new addition to the family of 2D materials besides semimetals (for example, graphene) and semiconductors (for example, MoS_2). Experimental work has revealed the existence of Dirac cones in β_{12} sheet,[6d] which lie at about 0.7 (2.0) eV along the ΓM (ΓX) direction in the Brillouin Zone (BZ) above the Fermi level. Moreover, theoretical works have demonstrated a variety of novel properties of borophenes, such as phonon-mediated superconductivity[5d,7], excellent mechanical behavior, and so on.[8] As a 2D ele-

[*] J. Zhang,[+] J. Zhang,[+] C. Cheng, Dr. C. Lian, J. Liu, Prof. S. Meng
Beijing National Laboratory for Condensed Matter Physics, and Institute of Physics Chinese Academy of Sciences
Beijing 100190 (P. R. China)
and
School of Physical Sciences
University of Chinese Academy of Sciences
Beijing 100049 (P. R. China)
E-mail: smeng@iphy.ac.cn
Dr. L. Zhou, Prof. S. Tretiak
Theoretical Division, Center for Nonlinear Studies and Center for Integrated Nanotechnologies, Los Alamos National Laboratory
Los Alamos, NM 87545 (USA)
Dr. J. Lischner
Departments of Materials and Physics, and the Thomas Young Centre for Theory and Simulation of Materials
Imperial College London
London SW7 2AZ (UK)
Prof. F. Giustino
Department of Materials, University of Oxford
Parks Road, Oxford OX1 3PH (UK)
[+] These authors contributed equally to this work.
Supporting information and the ORCID identification number(s) for the author(s) of this article can be found under: https://doi.org/10.1002/anie.201800087.

mental metal, the intrinsic electrical resistivity of borophene lies at the heart of its potential application in electronic devices and other boron-based nanodevices in the future. To our knowledge, experimental or theoretical investigations on the intrinsic electronic transport properties of borophene as a prototype 2D metal are still lacking.

Herein, we investigate the phonon-limited electric resistivity of 2D borophenes. First-principles calculations are performed within the Quantum ESPRESSO and EPW package.[9] Electronic transport properties are evaluated by the Ziman's resistivity formula.[9c] For β_{12} borophene, we use $30\times20\times1$ k-mesh in the full Brillouin integration for the charge density. The e-ph coupling matrix was calculated first on a coarse grid of $6\times4\times1$ mesh in BZ and then Wannier interpolated into an ultrafine grid of $300\times200\times1$ points (see the Supporting Information for more details).

Figure 1 shows atomic structures of boron sheets fabricated experimentally and the corresponding intrinsic resistivity $\rho_{e\text{-}ph}$ as the function of temperature in both linear and logarithmic scales. The β_{12} borophene is perfectly planar and has a rectangular primitive cell (lattice constants equal 2.93 Å and 5.07 Å). We see that $\rho_{e\text{-}ph}$ of β_{12} borophene is proportional to T^4 at low temperatures ($T<138$ K). This observation reflects the 2D nature of electrons and phonons in borophene. In contrast, $\rho_{e\text{-}ph}$ is linear in T when the temperature is larger than 138 K, with a slope of 0.016 μΩ cm K^{-1}. Therefore, the temperature dependence can be described well by the Bloch–Grüneisen model with $\Theta_{BG}=138$ K. This value is close to that estimated from the electronic and phonon band structures, $\Theta_{BG}\approx110$ K, further justifying the applicability of Bloch–Grüneisen model. At room temperature, the $\rho_{e\text{-}ph}$ of β_{12} borophene is 3.52 μΩ cm, being comparable to that of graphene (1.0 μΩ cm).[3] Another prominent feature of β_{12} borophene is the emergence of a transition at a very low temperature in resistivity scaling, as indicated in Figure 1 g.

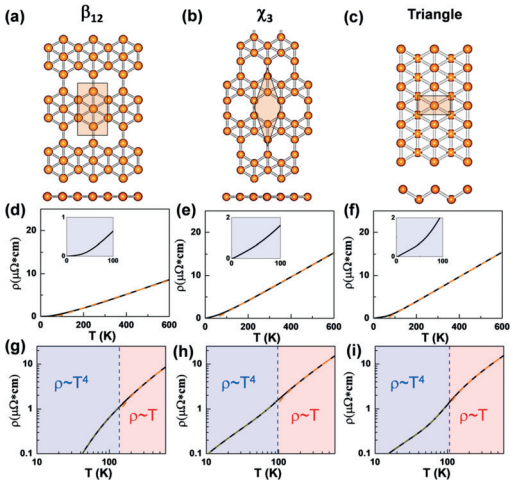

Figure 1. a)–c) Atomic structures of selected two-dimensional borophenes with the unit cells (top and side views). a) β_{12}, b) χ_3, c) triangle borophene. d)–f) Electrical resistivity of the three borophenes in linear scale (solid black lines). The insets (light blue regimes) in (d)–(f) show the resistivity at low temperatures. g)–i) Electrical resistivity in logarithmic scale. The vertical dashed lines in (d)–(i) indicate the crossover between two regions. Light red regions show $\rho\sim T$, while light blue regions indicate $\rho\sim T^4$.

For the χ_3 and triangle borophenes, similar trends for the $\rho_{e\text{-}ph}$ are observed (Figure 1 e,f). Furthermore, the $\rho_{e\text{-}ph}$ of the two borophenes is larger than that of the β_{12} phase: 6.68 and 6.82 μΩ cm at 300 K, respectively. To have a direct comparison of the transition point, the crossover from T^4 to T region is found to be at 97 K and 105 K for the χ_3 and triangle borophene, respectively (Figure 1 h,i). The Θ_{BG} of the three borophenes are all remarkably lower than the $\Theta_D=1700$ K (corresponding to the highest phonon energy, circa 1200 cm^{-1}). Therefore, we come to the first finding of this work: the temperature-dependent $\rho_{e\text{-}ph}$ of the borophenes are sensitive to their atomic structures, agreeing well with the Bloch–Grüneisen model with a Θ_{BG} of about 100 K.

In the following, we analyze the contributions of different phonon branches to the $\rho_{e\text{-}ph}$ of borophene. Here, we plot the total $\rho_{e\text{-}ph}$ of three polymorphs in logarithmic scale together with the contributions from different phonon modes (Figure 2). For β_{12} borophene, it is obvious that the contribution from the transverse acoustic mode (#2: TA, Figure 2 g) is the largest, accounting for about 30 % of the total $\rho_{e\text{-}ph}$ (300 K). The out-of-plane acoustic mode (#1: ZA, Figure 2 d) and transverse optical mode (#4: TO, Figure 2 j) with a frequency of 149 cm^{-1} at Γ point also play an important role in the $\rho_{e\text{-}ph}$, which are responsible for 20 % and 14 % of $\rho_{e\text{-}ph}$, respectively. Therefore, one can argue that acoustic phonon modes are the main resources of total $\rho_{e\text{-}ph}$ at low temperatures. However, the contribution of TO phonon mode cannot be ignored even at room temperature.

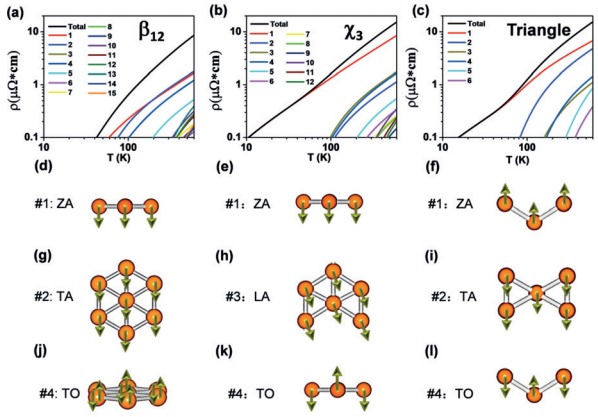

Figure 2. a)–c) The partial resistivity arising from each phonon branch for the three borophenes in logarithmic scale. d)–l) Atomic displacements of dominant phonon phonons. The sequences (#1, #2, etc.) are based on the relative energies of phonons. ZA, TA, LA, and TO indicate an out-of-plane acoustic, transverse acoustic, longitudinal acoustic, and transverse optical mode, respectively.

Different from β_{12} borophene, ZA phonon modes (#1 in Figure 2 e,f) of χ_3 and triangle borophenes contribute a dominant part in the total $\rho_{e\text{-}ph}$ (56 % and 44 %). It is clear that the optical phonon modes take up quite small fractions (ca. 5 % for both). It is reasonable since a higher excitation energy or much higher temperature is needed to excite the optical phonon modes. The fact that only low-energy phonons mainly

contribute to total $\rho_{e\text{-}ph}$ is direct evidence supporting the Bloch–Grüneisen behavior in the 2D metals.

For evaluating the intrinsic transport properties of 2D materials, deformation potential approximation (DPA) has been widely used, where only the LA phonons are considered to scatter carriers.[10] The method has been applied to some 2D materials; for example, graphene.[3b,11] However, our findings strongly suggest the failure of DPA for borophene, since the contributions from ZA and TA modes of borophene are important, similar to the cases of silicene and stanene.[11c]

Carrier density is an effective degree of freedom to manipulate electron–phonon interactions in 2D materials. Other than a conventional 3D material for which bulk carriers are far away from its surface and are easily screened by surface potential, a 2D metal has its surface fully exposed to an external gate; therefore the carrier density can be drastically tuned. As mentioned earlier, the phonon-limited resistivity of graphene is affected by carrier density, especially in the Θ_{BG} (changing from 100 K to 1000 K).[3] We notice that the charge doping effect from the silver substrates to β_{12} and χ_3 borophene is reported experimentally.[6b–d] Furthermore, Zhang et al. have reported that gate voltage is able to control the energy-favored boron sheets, offering new insights into the relative stability of borophenes at different doping levels.[5g] Therefore, an intriguing question arises on how much charge carriers can modulate the intrinsic electric resistivity of borophene.

We take β_{12} borophene as an example to tune the electric transport performance under high carrier densities (n). Figure 3 summaries the intrinsic electric resistivity of β_{12} borophene by adding additional electrons/holes ($n = \pm 2.0 \times 10^{14}$ cm^{-2} and $\pm 3.3 \times 10^{14}$ cm^{-2}). Here, we use "−" to represent electron doping and "+" to indicate hole doping. There is no imaginary phonon vibration for the carrier densities mentioned above, suggesting that the stability of 2D boron sheets can be preserved. Figure 3a presents the modulation in the $\rho_{e\text{-}ph}$ originating from varying dopant levels. As expected, $\rho_{e\text{-}ph}$ of three borophene polymorphs can be largely tuned by external charge carriers. In particular, we observe that hole doping may significantly increase electric resistivity. For $n = +2.0 \times 10^{14}$ cm^{-2}, the $\rho_{e\text{-}ph}$ of β_{12} borophene increased 1.76 times compared to that of pristine material (that is, from 3.52 to 5.78 μΩ cm at 300 K). Furthermore, this value grows to 15.10 μΩ cm (about 4.29 times over that of the pristine one) when the doping level increases to $n = +3.3 \times 10^{14}$ cm^{-2}. In contrast, election doping has lesser effect with relatively lower changes in $\rho_{e\text{-}ph}$ (that is, 2.16 and 1.17 times larger than that of pristine material at $n = -2.0 \times 10^{14}$ cm^{-2} and -3.3×10^{14} cm^{-2}, respectively).

To gain a quantitative analysis on the Bloch–Grünesisen behavior in β_{12} borophene at different densities, we fit $\rho_{e\text{-}ph}$ at two distinct regimes (Figure 3b). The crossover between the two regimes exhibits a small variation, ranging from 90 K to 138 K. These data suggest that the size of Fermi surface in borophene does not change appreciably when the ultrahigh carrier density is applied (see the Supporting Information). Despite the complex Fermi surface for β_{12} borophene, it can be argued that only some electron/hole pocket is mainly responsible for the intrinsic transport properties.[5h] Surprisingly, our result reflects that borophene is significantly different from graphene in the carrier-tuned transport behavior. The absolute value of $\rho_{e\text{-}ph}$ of borophene is highly sensitive to external carrier densities, while ultrahigh doping level in graphene leads to a relatively small variation in $\rho_{e\text{-}ph}$, owing to the cancellation of increasing carrier density and phonon scattering.

More information comes from the carrier-mediated band structures and phonon dispersions (Figure 4). Hole doping lowers the Fermi energy by 0.30 eV (0.43 eV) for $n = +2.0 \times 10^{14}$ cm^{-2} ($+3.3 \times 10^{14}$ cm^{-2}). More clearly, the $\alpha_{tr}^2F(\omega)$ exhibit a strong enhancement, which is a direct explanation for the large modulation in total $\rho_{e\text{-}ph}$ under different carrier densities.

Furthermore, the Θ_{BG} in borophene is nearly pinned around 100 K with varying carrier densities, while in graphene the Θ_{BG} changes dramatically, from 100 K to 1000 K with $n = 4 \times 10^{14}$ cm^{-2}. We present the normalized electrical resistivity ($\rho/\rho_{T=300\,K}$) of three borophenes and β_{12} sheet with different carrier densities (see the Supporting Information). It is obvious that the temperature-dependent resistivity of 2D metals observes a universal scaling:

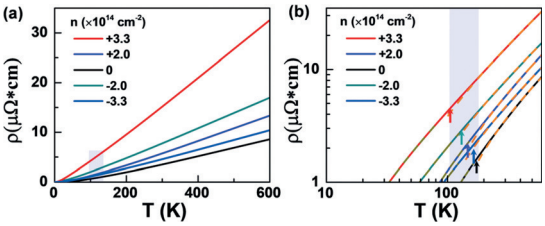

Figure 3. Electrical resistivity of β_{12} borophene with different charge carrier densities ($n = \pm 2.0 \times 10^{14}$ cm^{-2} and $\pm 3.3 \times 10^{14}$ cm^{-2}) a) in linear scale and b) in logarithmic scale. Solid lines are calculated from the first-principles method. Arrows in different colors are given to illustrate the transition points for two different transport behaviors.

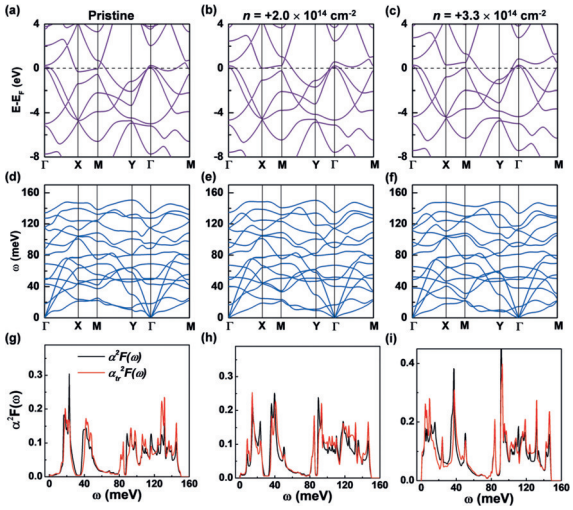

Figure 4. a)–c) Energy band structures of β_{12} borophene at different hole densities. Fermi levels are set to zero. d)–f) Phonon dispersions of β_{12} borophene at different hole densities. g)–i) Corresponding Eliashberg spectral function $\alpha^2F(\omega)$, along with the Eliashberg transport spectral functions $\alpha_{tr}^2F(\omega)$.

$$T < \Theta_{BG};\ \frac{\rho(T)}{\rho(T=300\,K)} = C_1 T^4$$
$$T > \Theta_{BG};\ \frac{\rho(T)}{\rho(T=300\,K)} = C_2 T + C_3 \quad (2)$$

where C_1 is on the order of about $10^{-8}/K^4$, C_2 is on the order of $10^{-3}\,K^{-1}$, and C_3 is about -0.3. In contrast to semimetals, 2D metals such as borophene are endowed with a high density of states at the Fermi level, which can accommodate high-density carrier doping without significant expansion of Fermi surface. The fixed Θ_{BG} upon doping and for distinct polymorphs suggest that the intrinsic resistivity of borophene follows a rather universal scaling behavior with temperature, for a large temperature range, which is desirable in many electronic applications.

We note that the ultrahigh carrier level discussed above is reasonable, which can be achieved for 2D systems in experiments, such as by an electrolytic gate or chemical absorption. In graphene, for example, extremely high carrier densities (up to $4.0\times10^{14}\,cm^{-2}$ for both electrons and holes) can be realized.[3a] Given that it is difficult to tailor the carrier concentration in traditional bulk metals, 2D borophene offers an excellent opportunity for realizing highly carrier-dependent electronic transport devices. Since borophenes can only exist on metallic substrates (for example, Ag) in recent experiments, we analyze the influence of substrates.[6a,b] A slight charge transfer (ca. 0.03 *e*/atom, or $1.0\times10^{14}\,cm^{-2}$) is found to take place from the silver substrate to the boron sheet, suggesting an increase in $\rho_{e\text{-}ph}$ by 10% when adsorbed on Ag substrate as compared to free-standing ones. At present the challenge in studying the transport properties of borophene lies in monolayer exfoliation from the substrates due to the relatively strong borophene–substrate interactions. However, with the development of advanced growth methods, we believe a freestanding borophene will be realized soon in experiments to validate the predictions reported above. The above findings may yield new device applications for borophenes: the high carrier-density sensitivity can be utilized for an external-gate regulated resistor or a memory resistor (memristor, in which the resistivity varies with the historical accumulated carrier density).[12]

To conclude, we employ ab initio calculations to investigate the phonon-limited resistivity of borophenes. Our study reveals the $\rho_{e\text{-}ph}$ magnitude of three borophene polymorphs can be greatly tuned with different polymorphs and carrier densities. We find that a Bloch–Grünesisen behavior with nearly pinned transition temperature (ca. 100 K) is broadly satisfied at different temperatures and carrier densities. These results suggest use of different doping methods to control the resistivity of boron-based 2D metals, thus facilitating future applications in 2D nanoelectronic devices.

Acknowledgements

This work was supported by National Key Research and Development Program of China (Grant Nos. 2016YFA0300902 and 2015CB921001), National Natural Science Foundation of China (Grant Nos. 11774396, 11474328 and 11290164), "Strategic Priority Research Program (B)" of Chinese Academy of Sciences (Grant No. XDB07030100), and Beijing Municipality (D161100002416003). The work at Los Alamos National Laboratory (LANL) was supported by the LANL LDRD program and was done in part at Center for Nonlinear Studies (CNLS) and the Center for Integrated Nanotechnologies (CINT).

Conflict of interest

The authors declare no conflict of interest.

Keywords: Bloch–Grüneisen model · borophene · electron–phonon coupling · intrinsic electrical resistivity

How to cite: *Angew. Chem. Int. Ed.* **2018**, *57*, 4585–4589
Angew. Chem. **2018**, *130*, 4675–4679

[1] a) F. Bloch, *Z. Phys.* **1930**, *59*, 208; b) E. A. Grüneisen, *Phys. (Leipzig)* **1933**, *16*, 530.
[2] a) M. S. Fuhrer, *Physics* **2010**, *3*, 106; b) E. H. Hwang, S. S. Das, *Phys. Rev. B* **2008**, *77*, 115449.
[3] a) D. K. Efetov, P. Kim, *Phys. Rev. Lett.* **2010**, *105*, 256805; b) C. H. Park, N. Bonini, T. Sohier, G. Samsonidze, B. Kozinsky, M. Calandra, F. Mauri, N. Marzari, *Nano Lett.* **2014**, *14*, 1113–1119; c) T. Y. Kim, C. H. Park, N. Marzari, *Nano Lett.* **2016**, *16*, 2439–2443.
[4] A. K. Geim, K. S. Novoselov, *Nat. Mater.* **2007**, *6*, 183.
[5] a) C. Ozdogan, S. Mukhopadhyay, W. Hayami, Z. Guvenc, R. Pandey, I. Boustani, *J. Phys. Chem. C* **2010**, *114*, 4362–4375; b) Z. Zhang, E. S. Penev, B. I. Yakobson, *Nat. Chem.* **2016**, *8*, 525; c) X. Wu, J. Dai, Y. Zhao, Z. Zhuo, J. Yang, X. C. Zeng, *ACS Nano* **2012**, *6*, 7443; d) E. S. Penev, S. Bhowmick, A. Sadrzadeh, B. I. Yakobson, *Nano Lett.* **2012**, *12*, 2441–2445; e) Y. Liu, E. S. Penev, B. I. Yakobson, *Angew. Chem. Int. Ed.* **2013**, *52*, 3156; *Angew. Chem.* **2013**, *125*, 3238; f) Z. Zhang, Y. Yang, G. Gao, B. I. Yakobson, *Angew. Chem. Int. Ed.* **2015**, *54*, 13022; *Angew. Chem.* **2015**, *127*, 13214; g) Z. Zhang, S. N. Shirodkar, Y. Yang, B. I. Yakobson, *Angew. Chem. Int. Ed.* **2017**, *56*, 15421–15426; *Angew. Chem.* **2017**, *129*, 15623–15628; h) E. S. Penev, A. Kutana, B. I. Yakobson, *Nano Lett.* **2016**, *16*, 2522.
[6] a) A. J. Mannix, X.-F. Zhou, B. Kiraly, J. D. Wood, D. Alducin, B. D. Myers, X. Liu, B. L. Fisher, U. Santiago, J. R. Guest, *Science* **2015**, *350*, 1513; b) B. Feng, J. Zhang, Q. Zhong, W. Li, S. Li, H. Li, P. Cheng, S. Meng, L. Chen, K. Wu, *Nat. Chem.* **2016**, *8*, 563–568; c) Z. Zhang, A. J. Mannix, Z. Hu, B. Kiraly, N. P. Guisinger, M. C. Hersam, B. I. Yakobson, *Nano Lett.* **2016**, *16*, 6622–6627; d) B. Feng, O. Sugino, R.-Y. Liu, J. Zhang, R. Yukawa, M. Kawamura, T. Iimori, H. Kim, Y. Hasegawa, H. Li, L. Chen, K. Wu, H. Kumigashira, F. Komori, T. C. Chiang, S. Meng, I. Matsuda, *Phys. Rev. Lett.* **2017**, *118*, 096401.
[7] a) M. Gao, Q. Li, X. W. Yan, J. Wang, *Phys. Rev. B* **2017**, *95*, 024505; b) C. Cheng, J. Sun, H. Liu, H. Fu, J. Zhang, X. Chen, S. Meng, *2D Mater.* **2017**, *4*, 025032.
[8] a) X. Sun, X. Liu, J. Yin, J. Yu, Y. Li, Y. Hang, X. Zhou, M. Yu, J. Li, G. Tai, *Adv. Funct. Mater.* **2017**, *27*, 19; b) Z. H. Cui, E. Jimenez-Izal, A. N. Alexandrova, *J. Phys. Chem. Lett.* **2017**, *8*, 1224–1228; c) Z. Zhang, Y. Yang, E. S. Penev, B. I. Yakobson, *Adv. Funct. Mater.* **2017**, *27*, 1605059; d) Y. Huang, S. N. Shirodkar, B. I. Yakobson, *J. Am. Chem. Soc.* **2017**, *139*, 17181–17185; e) L. Adamska, S. Sadasivam, Foley, J. Jonathan, P. Darancet, S. Sharifzadeh, *J. Phys. Chem. C* **2018**, *122*, 4037–4045; f) M. Ezawa, *Phys. Rev. B* **2017**, *96*, 035425.

[9] a) P. Giannozzi, et al., *J. Phys. Condens. Matter.* **2009**, *21*, 395502; b) S. Poncé, E. R. Margine, C. Verdi, F. Giustino, *Comput. Phys. Commun.* **2016**, *209*, 116 – 133; c) J. Ziman, *Electrons and Phonons*, Oxford University Press, Oxford, **1960**.
[10] J. Bardeen, W. Shockley, *Phys. Rev.* **1950**, *80*, 72.
[11] a) K. Kaasbjerg, K. S. Thygesen, K. W. Jacobsen, *Phys. Rev. B* **2012**, *85*, 165440; b) Y. Cai, G. Zhang, Y. W. Zhang, *J. Am. Chem. Soc.* **2014**, *136*, 6269 – 6275; c) Y. Nakamura, T. Zhao, J. Xi, W. Shi, D. Wang, Z. Shuai, *Adv. Electron. Mater.* **2017**, *3*, 1700143.
[12] D. B. Strukov, G. S. Snider, D. R. Stewart, R. S. Williams, *Nature* **2008**, *453*, 80 – 83.

Manuscript received: January 4, 2018
Revised manuscript received: February 1, 2018
Accepted manuscript online: February 27, 2018
Version of record online: March 14, 2018

